Three-center-four-electron halogen bond enables sub-ppm-level non-metallic complex catalysis

Shunya Oishi,[†,‡,§] Takeshi Fujinami,[†,§] Yu Masui,[†,‡] Toshiyasu Suzuki,[†] Masayuki Kato,[†,‡] Naoya Ohtsuka,[†,‡] and Norie Momiyama[†,‡]*

[†]Institute for Molecular Science, Okazaki, Aichi 444-8787, Japan
[‡]SOKENDAI (The Graduate University for Advanced Studies), Okazaki, Aichi 444-8787, Japan
[§]These two authors contributed equally.

*e-mail: momiyama@ims.ac.jp

ABSTRACT:

The three-center-four-electron halogen bond (3c4e X-bond) presents a new design concept for catalysis. By integrating halogen(I) (X^+: I^+ or Br^+), bis-pyridyl ligand *NN*, and non-nucleophilic counter anion Y. [*N*···X···*N*]SbF_6, we developed non-metallic complex catalysts, [*N*···X···*N*]Ys, which exhibited outstanding activity and facilitated the Mukaiyama–Mannich-type reaction of *N*-heteroaromatics with sub-ppm-level catalyst loading. The high activity of [*N*···X···*N*]SbF_6 was clearly demonstrated. NMR titration experiments, CSI-MS, computations, and UV-vis spectroscopic studies attribute the robust catalytic activity of [*N*···X···*N*]Y to the unique feature of the 3c4e X-bond for binding chloride: i) the partial covalent nature transforms [*N*···X···*N*]$^+$ complexation to sp^2CH as a hydrogen bonding donor site, and ii) the noncovalent property allows for the dissociation of [*N*···X···*N*]$^+$ for the formation of [Cl···X···Cl]$^-$. This study introduces a new application of 3c4e X-bonds to catalysis via halogen(I) complexes.

TEXT:

Organocatalysts are a 21st century development in the field of catalysis. The design of organic molecules and ionic species as catalysts has advanced remarkably over the past two decades, and these catalysts are now useful facilitators of various chemical reactions.[1–11] *In situ*-generated reactive intermediates through covalent bond formations involving noncovalent interactions are essential to promoting the reaction in organocatalysis. The hydrogen bond (H-bond) is the most frequently applied noncovalent interaction in organocatalysis, and is the reason underlying the prominent success in the development of organocatalysis.[12–15]

The halogen bond (X-bond) in solution[16–21] has recently drawn considerable attention owing to the similarity of its electrostatic property to that of the H-bond in solution. The two-center-two-electron (2c2e) bond-based interactions are the most common features in both the H- and X-bonds: the positive charge of a hydrogen atom or a small region of positive charge on the terminus of a halogen atom can interact with the negative charge of an electron-rich species (Fig. 1). Therefore, X-bond-based organocatalysts have been developed and become rapidly widespread as a new research area of organocatalysis.[22–27] In 2008, Bolm et. al. reported organocatalysis through X-bond activation using haloperfluoroalkanes for the first time.[28] Three years after Bolm's report, Huber et. al. designed X-bond-based organocatalysts using perfluorinated iodoterphenyls and their analogs with the ability to facilitate the carbon–carbon bond forming reaction for the first time.[29] Soon after this seminal report, Huber et. al.,[30] Tan et. al.,[31] Takemoto et. al.,[32] and Takeda et. al.[33] independently developed azolium-based cationic X-bond donor catalysts that are currently identified as being essential to the achievement of relatively strong X-bond donor abilities. Moreover, iodine(III) species, such as diaryliodonium and cyclic iodolium compounds, were introduced as organocatalysts with an X-bond donor site.[34–39] Based on these remarkable contributions, chiral molecules with X-bond donor sites for asymmetric catalysis were reported by Huber,[40] Arai,[41–43] Tan,[44] Yeung,[45] Mancheño,[46] and Yoshida[47]. These achievements constantly focus on the "classical" 2c2e X-bond donor sites where one halogen atom involves one Lewis basic site to generate reactive electrophilic species.

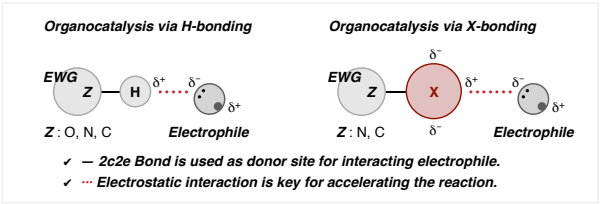

Fig. 1. Schematics of the "classical" two-center-two-electron (2c2e) bond in hydrogen-bond and halogen bond-based organocatalysis.

Although the features of the halogen atom of the "classical" 2c2e X-bond exhibit similarities with the hydrogen atom as the donor site of electrostatic interaction, the distinct formation of the three-center-four-electron (3c4e) bond is unique to the halogen atom. Although the 3c4e bond in the H-bond has been discussed and utilized in the design of H-bond-based organocatalysis,[48–52] its structure (2c2e or 3c4e bond) continues to be ambiguous (Fig. 2a, left).[53–59] In contrast with the H-bond, the chemical and physical properties of the 3c4e X-bond have been clearly and extensively demonstrated in numerous studies over the past few decades. Halogen(I), generally X^+ (X = I, Br, Cl), acts as a strong X-bond donor site, where one halogen concurrently interacts with two Lewis bases (Fig. 2a,

right).[60–63] Either the cationic or anionic 3c4e bond would be formed depending on the neutral Lewis base or anion as the X-bond acceptor, which is in contrast with those of the "classical" 2c2e X-bond. In particular, Erdélyi, who developed a [1,2-bis(pyridine-2-ylethynyl)benzene] iodine(I) complex, is a pioneer in the redefinition of the 3c4e X-bond. In addition, the derivatives and unique features of the 3c4e X-bond were revealed using NMR spectroscopy, density functional theory (DFT) calculations, and X-ray crystal analysis (Fig. 2b).[64–77] Otherwise, cationic 3c4e X-bond complexes have frequently been utilized in organic syntheses: one of the representatives is [bis(pyridine)halogen(I)]$^+$ tetrafluoroborate, also called Barluenga's reagent, which has been used in halogenation, cyclization, and oxidation.[78,79] In 2014, Takemoto et. al. demonstrated the potential of Barluenga's reagent as a promoter, where the stoichiometric amount of Barluenga's reagent facilitated desilylative semipinacol rearrangement of halohydrin silyl ethers in moderate yield (Fig. 2c, top).[80] For the anionic 3c4e X-bond, Minakata et al. demonstrated the utility of the triiodide species in synthetic organic chemistry, which played a crucial role as the radical resource for promoting the reaction of alkenes with *N*,*N*-diiodotosylamide dramatically (Fig. 2c, bottom).[81] Despite the utility of the 3c4e X-bond in synthetic chemistry, very little attention has been paid to the 3c4e X-bond complexes as molecular catalysts.

To the best of our knowledge, the potential of 3c4e complexes as non-metallic complex catalysts has not been fully investigated. This may be attributed to the focus of spectroscopy and computational studies on the structures of supramolecular complexes of the 3c4e X-bonds; they are not regarded as transformative chemical species through the selection of 3c4e X-bond acceptors. Therefore, we focus on the partial covalent and total noncovalent features of the 3c4e X-bond to strategically design non-metallic complex catalysts and particularly develop anion-binding catalysts (Fig. 2d).[82–86] We envisaged that the cationic [*N*···X···*N*]$^+$ bond-assisted H-bonding interaction would assemble anion Z^-, such as chloride, at the initial stage of catalysis, and then electrophilic halogen X of the [*N*···X···*N*]Ys complex would be subjected to nucleophilic attack by anion Z^- to transform the anionic [*Z*···X···*Z*]$^-$ bond through ligand exchange from bis-pyridine to anion Z^-, which becomes a driving force in anion-binding catalysis (Fig. 2e).

We report herein the development of bis-pyridine halogen(I) complexes **1** ([*N*···X···*N*]Ys; *N* is substituted pyridine, X is I or Br; Y is a non-nucleophilic counter anion) as halonium complex catalysts, thus demonstrating the viability of our design concept for highly active anion-binding catalysis. [*N*···X···*N*]Ys exhibits robust activity (up to 500 ppm catalyst loading, 0 °C, 1 h) and a broad substrate scope (18 examples) in the Mukaiyama–Mannich-type reaction of *N*-hetero aromatics. Furthermore, we provide evidence for the dissociation, formation, and reformation of cationic and anionic X-bonds, *i.e.*, [*N*···X···*N*]$^+$ + 2Cl$^-$ ⇄ [Cl···X···Cl]$^-$ + *NN* (X is I, Br; *NN* is pyridyl ligand), through NMR titration experiments, CSI-MS, DFT calculations, and UV-vis spectroscopic studies. Our catalysis

design using the 3c4e X-bond addresses the limitation of catalytic activity in the previous H-bond based anion-binding catalysis, thereby allowing for high reaction efficiency with sub-ppm-level catalyst loading.

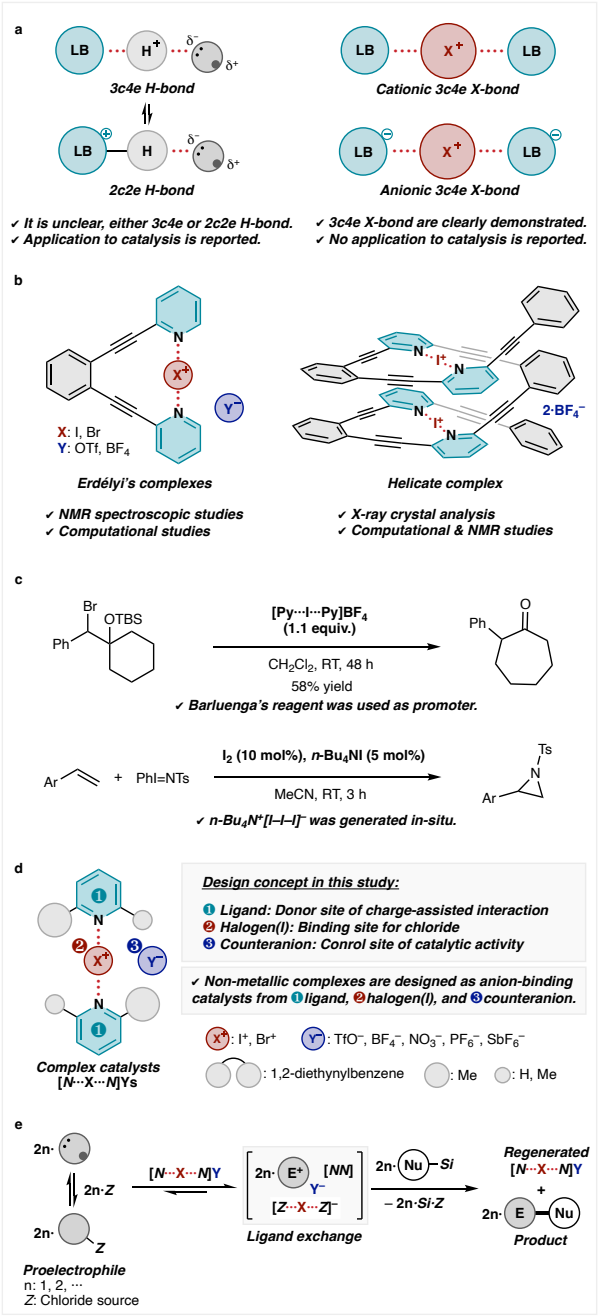

Fig. 2 Schematic of the three-center-four-electron (3c4e) bond and related information. a). Comparison of the 3c4e X-bond with the 3c4e H-bond. **b).** Erdélyi's complexes and their helicates. **c).** Recent application of the 3c4e bond in organic synthesis. **d).** Our design concept of the 3c4e bond complex catalysis. **e).** Working hypothesis, E^+ indicates an electrophilic species, Nu-*Si* indicates a nucleophile, and *Z* indicates a chloride source.

Results and discussion

Synthesis of halogen(I) complex catalysts. Initially, a variety of halogen(I) complex catalysts were synthesized according to the reported procedure.[64] Among them, 1,2-bis(pyridine-2-ylethynyl)benzene iodine(I) triflate (**1a**), Erdélyi's complex, was used as the benchmark complex catalyst as it was easy to handle owing to complex stability. Moreover, two types of protonated **L1** triflates were prepared as references to prevent H^+ from contaminating **1a** (Supporting Information).[69,87] We confirmed that ^{1}H NMR spectra of **1a** were significantly different from those of the protonated **L1**, which clearly showed our synthesized **1a** iodine complex without the contamination of protonated complexes. All complex **1s** were synthesized and characterized accordingly. Therefore, we used complex **1** as the halogen(I) complex catalyst for further studies.

Determination of target reaction. To prove our working hypothesis of the 3c4e X-bond complexes as anion-binding catalysts, we determined the primary target based on scatter plots of the yields (%) *vs.* catalyst loading (mol%) (Supporting Information). For this purpose, the Mukaiyama–Mannich-type reaction of *N*-heteroaromatics *via* chloride-binding was selected because the reaction provides a variety of useful nitrogen-containing intermediates for the synthesis of pharmaceuticals.[88–92] To generate scatter plots, data sets were prepared from 396 reactions of previously reported H-bond and X-bond-based anion-binding catalysts, particularly chloride-binding.[93–106] Of the representative *N*-heteroaromatics, *i.e.,* isoquinolines, quinolines, and pyridines, the success of catalytic processes for the reaction of pyridines was significantly limited. Therefore, the Mukaiyama–Mannich-type reaction of pyridine compounds **2**, chloroformates **3**, and silyl enol ethers **4** was examined for our initial study.

Reaction optimization. In our initial studies, we started with pyridine (**2a**), phenyl chloroformate (**3a**), and silyl ketene acetal **4a** at 0 °C for 1 h with or without **1a** (Table 1). The primary examinations revealed that 10 mol% of **1a** efficiently accelerated the reaction, thus excellently yielding γ-adduct **5a** (entry 1 vs. 2). Despite the lower catalyst loading of **1a**, such as 2.5, 1.0, 0.1, and 0.05 mol% (500 ppm), the reaction proceeded smoothly, producing reasonable yields of **5a** (entries 3, 4, 5, and 6). For comparison, 1,3-bis[3,5-bis(trifluoromethyl)phenyl] thiourea (Schreiner's thiourea catalyst)[107] and 1,3-bis(1-(3,5-bis(trifluoromethyl)-phenyl)-1H-1,2,3-triazol-4-yl)benzene (mother skeleton of Mancheño's bis-triazole catalyst)[95,96,101,103,104,106,108] were examined as the representative of the H-bond based anion-binding catalysts. Both catalysts were unable to considerably accelerate the reaction to produce high yields of **5a** (entries 7 and 8). Whereas iodoimidazolium triflate and dibenzoiodolium triflate were recently recognized as strong 2c2e X-bond donor catalysts (entries 9 and 10), their activities were comparable to that by **1a**.

Otherwise, *N*-methylated pyridyl triflate ([2Me·**L1**]·2OTf) accelerated the reaction,[109] but yielded 10% less **5a** than the corresponding iodine(I)complex **1a** (entry 11). Overall, these control experiments indicated the potential of catalyst design using halogen(I) complex **1**. Next, to establish the utility of **1** as the 3c4e-X-bond-based catalyst system, various counteranions, the change in halogen(I), and the other pyridyl ligands were examined. Screening of counter anions (entries 12–17) showed that antimonate complex **1e** produced the highest yield (90%) of product **5a**, even with 0.1 mol% catalyst loading (entry 15). Notably, a similar high yield (82%) and a satisfactory yield (74%) were obtained even when **1e** was reduced to 0.050 mol% (= 500 ppm), and further to 0.025 mol% (= 250 ppm) (entries 16 and 17) respectively, while 100 ppm catalyst loading only produced a moderate yield (entries 18). Bromine(I) antimonate complex **1f**, and iodine(I) complexes **1g**, **1h**, and **1i** with other pyridyl ligands—**L2**, **L3**, and **L4**—could be applied to achieve higher yields than that in the case of **1e**. Although the handling of these catalysts was complicated by the low stability of the complexes, high yields similar to those of **5a** were obtained (entries 19–22). Although inorganic compounds, iodine monochloride (ICl), and elemental iodine (I_2) accelerated the reaction, the product yields of **5a** were lower than that in the case of **1e** (entries 16 *vs.* 23 and 24). To exclude the possibility of hidden acids being real catalyst species that resulted from moisture during the adjustments, the reactions were conducted in tetrahydrofuran (THF) with 1 wt% or 5 wt% of H_2O; no reactions were observed (entries 25 and 26). These results demonstrated that [*N*···X···*N*]Ys, composed of pyridyl ligand, halogen(I), and non-nucleophilic counteranion, plays a significant role in efficiently promoting the reaction.

Table 1. Evaluation of the catalytic activity of [*N*···X···*N*]Y in the Mukaiyama–Mannich-type reaction[a]

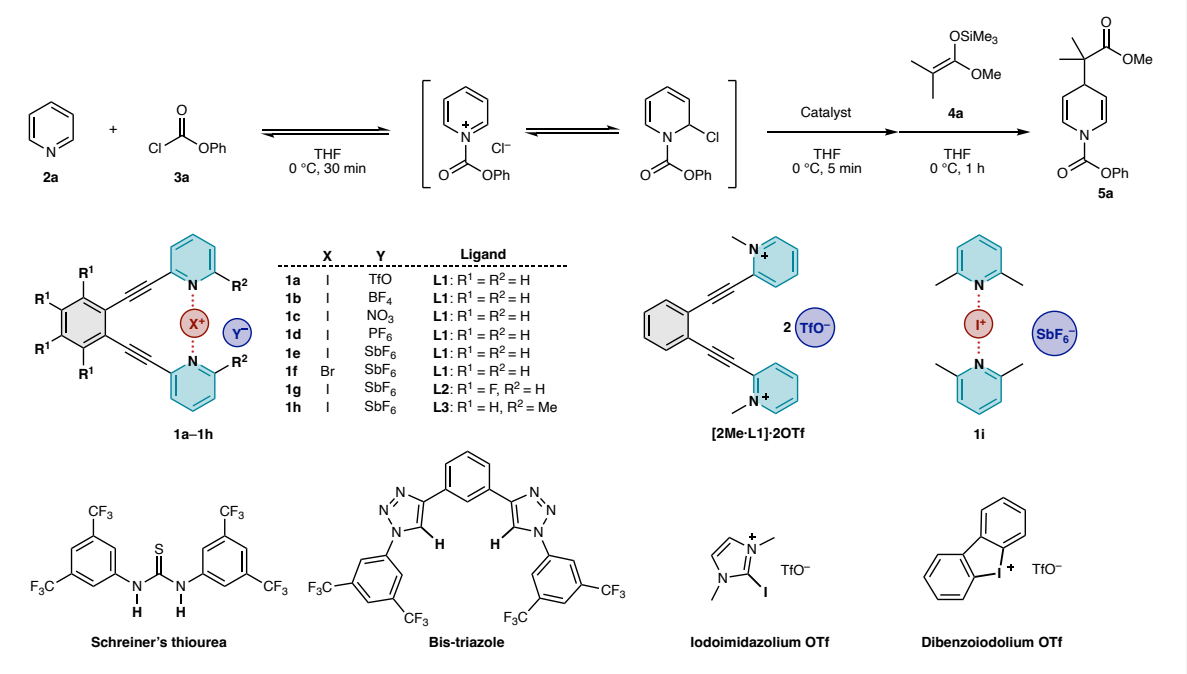

Entry	Catalyst (mol%)		Yield (%)[b]
1	**1a**	(10)	98
2	None	—	33
3	**1a**	(2.5)	90
4	**1a**	(1.0)	90
5	**1a**	(0.10)	76
6	**1a**	(0.050=500 ppm)	61
7	Schreiner's thiourea	(0.050=500 ppm)	33
8	Bis-triazole	(0.050=500 ppm)	49
9	Iodoimidazolium OTf	(0.050=500 ppm)	62
10	Dibenzoiodolium OTf	(0.050=500 ppm)	61
11	[2Me·**L1**]·2OTf	(0.050=500 ppm)	49
12	**1b**	(0.10)	49
13	**1c**	(0.10)	49
14	**1d**	(0.10)	87
15	**1e**	(0.10)	90
16	**1e**	(0.050=500 ppm)	82
17	**1e**	(0.025=250 ppm)	74
18	**1e**	(0.010=100 ppm)	52
19	**1f**	(0.050=500 ppm)	87
20	**1g**	(0.050=500 ppm)	87
21	**1h**	(0.050=500 ppm)	72
22	**1i**	(0.050=500 ppm)	87

23	ICl	(0.05=500 ppm)	51
24	I_2	(0.05=500 ppm)	60
25	**1e** + 1 wt% H_2O	(0.05=500 ppm)	<1
26	**1e** + 5 wt% H_2O	(0.05=500 ppm)	<1

[a] Reactions were run with pyridine (**2a**) (0.4 mmol), phenyl chloroformate (**3a**) (0.42 mmol), and ketene silyl acetal **4a** (0.6 mmol) in the presence of a catalyst for 1 h in tetrahydrofuran (THF; 8 mL). [b] Isolated yields.

Scope of 3c4e X-bond-based anion-binding catalysis. Following the acquisition of the easy-to-handle and optimal complex catalyst **1e**, the scope of the Mukaiyama–Mannich-type reaction was examined (Fig. 3a). The reactions of **2a** with β-disubstituted silyl ketene acetals, **4a**, **4b**, and **4c,** were accelerated in the presence of 500 ppm of **1e** and high yields of products **5a**, **5b**, and **5c,** respectively, were obtained with γ-selectivities. In particular, highly reactive and unstable **4c** reacted seamlessly to complete the reaction at –78 °C within 15 min. The reaction of **2a** with β-unsubstituted silyl ketene acetals **4d** and **4e** produced remarkable yields of **5d**, along with a mixture of α- and γ-products, regardless of the silyl substituents. Unfortunately, **1e** did not show any catalytic activity in the reaction of silyl enol ether **4f**. Other chloroformates such as **3b**, **3c**, and **3d** were also adequately tolerated in this reaction. Although higher catalyst loadings of 0.1–1.0 mol% were required for 2-, 3-, and 4-substituted pyridines **2b**–**2i** owing to the substitution effect for the reactivity of pyridinium substrates, moderate to high yields were obtained in the presence of **1e**. In the cases that involved α/γ selectivity, the product regioselectivities of **5a**–**5m** were provided according to the electron density of nucleophilic carbon in **4**; otherwise, **5n**–**5p** depended on the influence of pyridinium salt. In all cases, **1e** affected the reaction acceleration, but did not involve α/γ selectivity. The **1e** catalyst system also tolerated the reaction of quinoline, isoquinoline, and dihydroxyisoquinoline to yield corresponding products **5q**, **5r**, and **5s**. To clearly demonstrate the robustness of the [*N*···X···*N*]Ys catalyst system, all experimental data in the primary study and reaction scope were plotted on previously reported 396 reaction data of the yields (%) *vs.* catalyst loading (mol%) for the Mukaiyama–Mannich-type reaction of *N*-heteroaromatics *via* chloride-binding (Fig. 3b). The [*N*···X···*N*]Ys catalyst system realized relatively high yield with relatively low catalyst loading than the previously reported system in all cases, which addressed the drawback of catalytic activities in anion-binding catalysis.

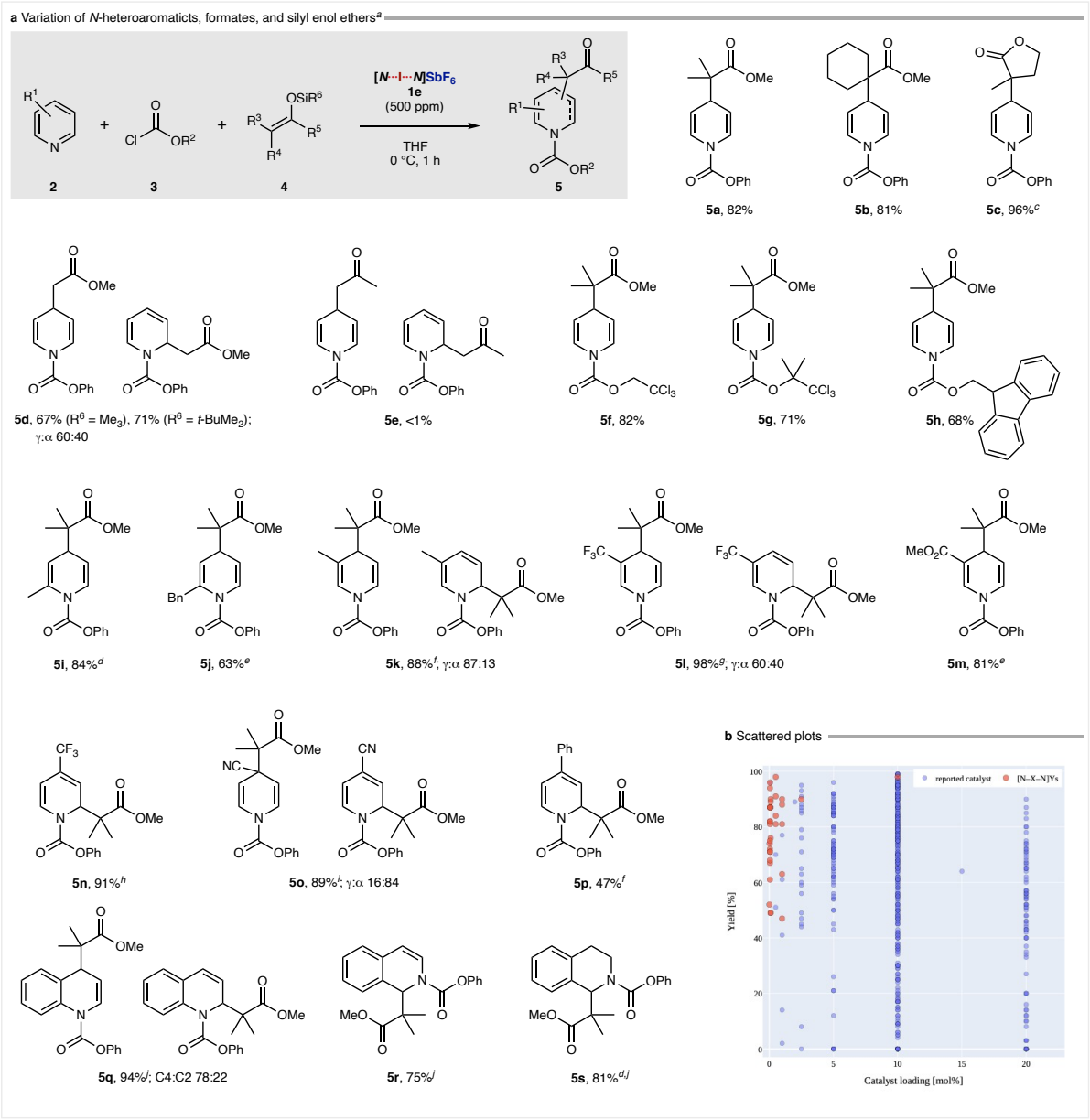

Fig. 3 Scope of 1e-catalyzed Mukaiyama–Mannich-type reaction[a] a). Variation of *N*-heteroaromatics, formates, silyl enol ethers. **b)** Scattered plots between the yields (%) *vs.* catalyst loading (mol%), and color separated with respect to [*N*···X···*N*]Ys catalyst system and reported system. [a] Unless otherwise noted, reactions were run with **2** (0.4 mmol), **3** (0.42 mmol), **4** ($R^6 = Me_3$, 0.6 mmol), **1e** at 0 °C for 1 h in THF (8 mL). [b] Isolated yields. [c] –78 °C, 15 min. [d] 0.5 mol% **1e**, 0.4 M solution. [e] 1.0 mol% **1e**, [f] 1.0 mol% **1e**, 0.4 M solution. [g] 0.5 mol% **1e**, 3 h, 0.1 M solution. [h] 0.5 mol% **1e**, 0.1 M solution. [i] 0.1 mol% **1e**, 0.1 M. [j] –40 °C, 3 h.

X-ray diffraction analysis of 3c4e X-bonds. As mentioned in previous reports,[110–116] Cl–I–N and Cl–I–Cl bonds were found in the crystal structures of halide complexes; therefore, we preliminarily performed X-ray diffraction analysis to demonstrate the formation of

[*N*···X···*N*]$^+$ to [Cl···X···Cl]$^-$. Although co-crystallization was not accomplished with the mixture of any [*N*···X···*N*]Ys and chloride source such as *n*-Bu$_4$NCl, certain halide complexes were fortunately obtained from **L1**, **L2**, and ICl (Fig. 4). The X-ray crystal packing of **L1** and ICl complex suggests a **L1** ligand to ICl ration of 1:2, *i.e.* [Cl···I···*NN*···I···Cl] complex (Fig. 4a). For the crystals obtained from **L2** ligand and ICl, two kinds of complexes, a 1:1 [^{F4}*N*···I···*N*][Cl···I···Cl] complex (Fig. 4b) and a 1:2 **L2** ligand to ICl complex, *i.e.* [Cl···I···^{F4}*NN*···I···Cl] complex (Fig. 4c), were observed. These structures show the possibility of dissociation from [*N*···X···*N*]Y to [*NN*···I]$^+$···Cl$^-$ and further transformation to [Cl···I···Cl]$^-$ in the presence of excess chloride.

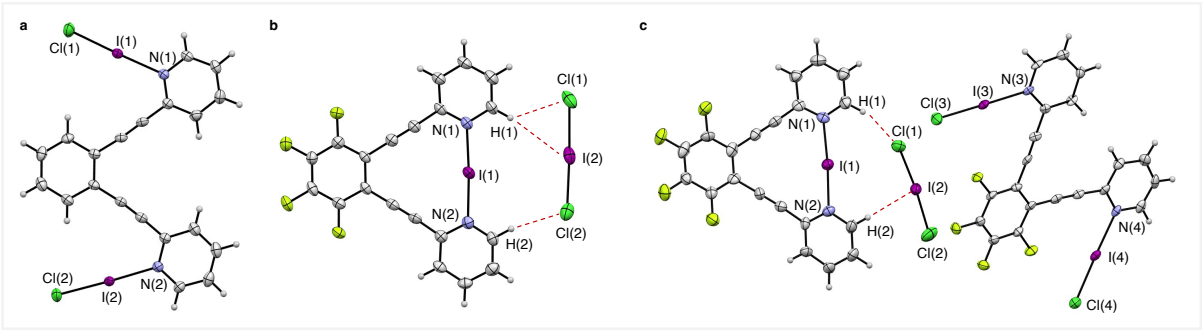

Fig. 4. X-ray diffraction analysis. a). 1:2 **L1** to ICl complex [Cl–I–*NN*–I–Cl]. **b).** 1:1 **L2** to ICl complex [^{F4}*N*–I–*N*][Cl–I–Cl]. **c).** Twin crystal of [^{F4}*N*–I–*N*][Cl–I–Cl] and [Cl–I–^{F4}*NN*–I–Cl].

Mechanistic studies. Based on X-ray crystal structures indicating the bond formation of Cl···I···N and [Cl···I···Cl]$^-$, ^{1}H NMR and CSI-MS measurements were undertaken using **1e** to gain insight into the binding modes of **1** to Cl$^-$ in the solution (Fig. 5). Three phases of peak changes were observed during ^{1}H NMR titration (Fig. 5a): i) In the cases where 0.1 to 1.0 equiv. of *n*-Bu$_4$NCl was added, aromatic peaks of **1e**—green-filled dots—shifted downfield, were observed, showing a trend similar to that in the report by Berkessel et al.[30] Furthermore, new broad aromatic peaks—blue-filled dots—as well as sharp aliphatic peaks—red-filled dots—gradually appeared. ii) In cases where 1.0 to 2.0 equiv. of *n*-Bu$_4$NCl was added, sharp aromatic peaks of **1e**—green-filled dots—gradually decreased in size and completely disappeared in the 2 equiv. of *n*-Bu$_4$NCl. Moreover, broad aromatic peaks—blue-filled dots—as well as sharp aliphatic peaks—red-filled dots—gradually increased in size. iii) In cases where more than 2 equiv. of *n*-Bu$_4$NCl was added, broad aromatic peaks—blue-filled dots—shifted upfield and were sharpened. Conversely, sharp aliphatic peaks—red-filled dots—shifted downfield and gradually increased in size. CSI-MS spectra show four peaks at *m*/*z* = 719.5, 522.4, 407.0, and 242.3 in the positive mode, and two peaks at *m*/*z* = 234.9 and 196.9 in the negative mode in the 1:1 mixture of **1e** and *n*-Bu$_4$NCl (Fig. 5b). These peaks correspond to the **L1**·*n*-Bu$_4$N$^+$·[Cl···I···Cl]$^-$, [**L1**·*n*-Bu$_4$N]$^+$,

[**L1**·I]$^+$, [*n*-Bu$_4$N]$^+$, SbF$_6^-$, and [Cl···I···Cl]$^-$, respectively. Peak intensity of [**L1**·I]$^+$ in the 1:1 mixture is significantly stronger than that of **L1**·*n*-Bu$_4$N$^+$·[Cl···I···Cl]$^-$ following the addition of 0.5 equiv. of *n*-Bu$_4$NCl to **1e**. In contrast, when a solution with **1e** and *n*-Bu$_4$N$^+$ in a 1:2 ratio was applied, the peak of [**L1**·I]$^+$ disappeared, whereas the peak of **L1**·*n*-Bu$_4$N$^+$·[Cl···I···Cl]$^-$ was maintained. These spectral changes strongly support the following chloride-binding mode using complex catalyst **1**: i) [*N*···X···*N*]Y + *n*-Bu$_4$NCl ⇄ [*N*···X···*N*]$^+$···Cl$^-$ + *n*-Bu$_4$N$^+$···Y$^-$, and ii) [*N*···X···*N*]$^+$···Cl$^-$ + *n*-Bu$_4$NCl ⇄ [*NN*]···*n*-Bu$_4$N$^+$ + [Cl···X···Cl]$^-$.

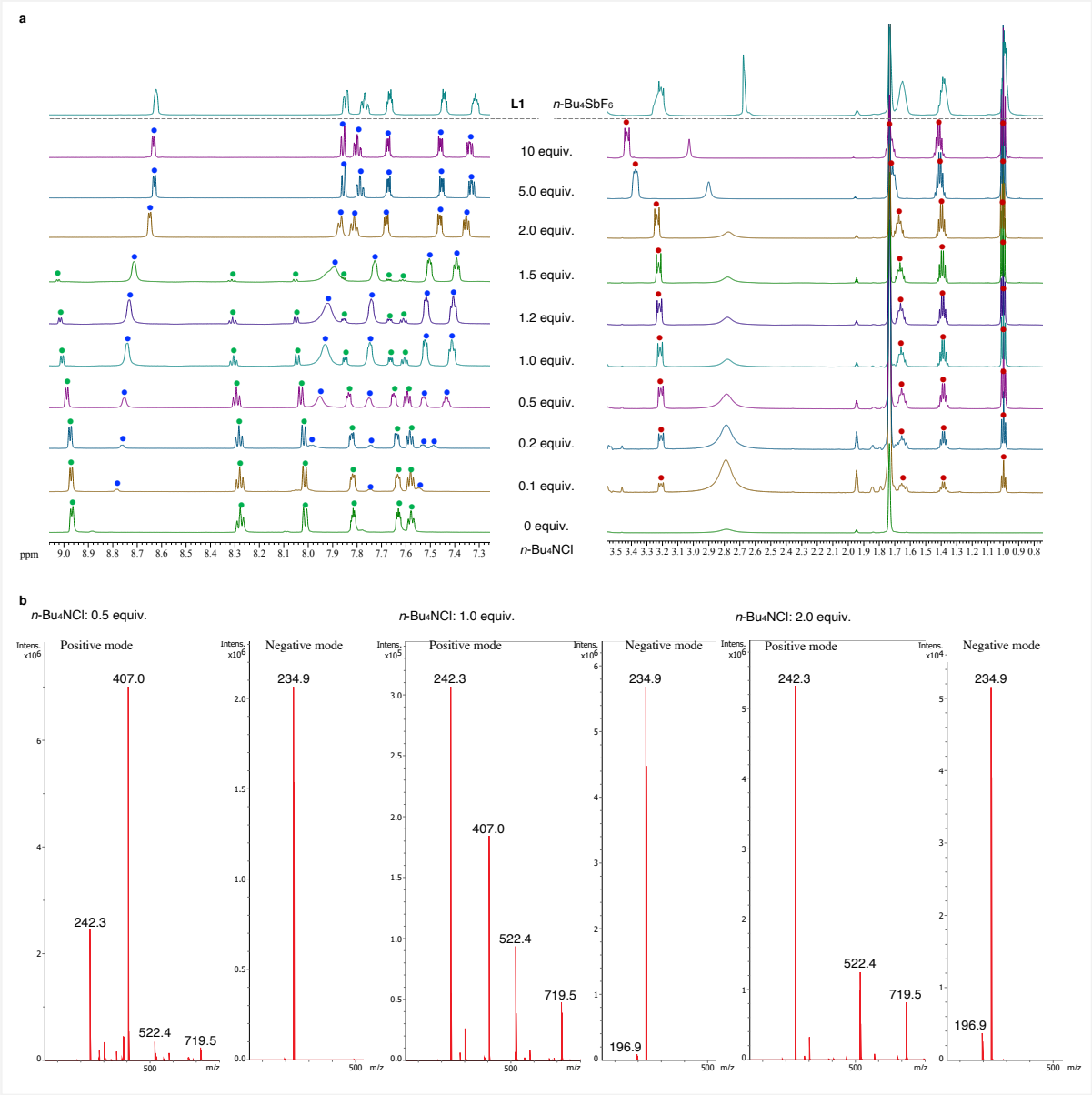

Fig. 5. Mechanistic studies with *n*-Bu$_4$NCl as chloride source. a). NMR and **b).** CSI-MS titration experiment on [*N*···I···*N*]SbF$_6$ (**1e**) and *n*-Bu$_4$NCl. The titration of [*N*···I···*N*]SbF$_6$

(**1e**) against *n*-Bu_4NCl; THF-d8/CD_3CN 9:1 (*v*/*v*), 0 °C for NMR; THF/CH_3CN 9:1 (*v*/*v*), –20 °C for CSI-MS.

Considering these experimental studies including X-ray diffraction analyses, we proposed the catalytic cycle shown in Fig. 6. In this mechanism, the sp^2CH next to ligand nitrogen in **1e** would initially interact with chloride, and then the nucleophilic attack of chloride on halogen(I) would cause the formation of N···X^+···Cl^- followed by [Cl···X···Cl]$^-$ bonds. Both [*N*···X···*N*]$^+$ the charge-assisted sp^2CH-bond and [Cl···X···Cl]$^-$ anionic 3c4e X-bond should be synergistically involved to generate electrophilic **2**·**3**$^+$ species. The resulting **2**·**3**$^+$ would be subjected to the nucleophilic attack by silyl enol ether **4** to yield the silylated intermediate yielding product **5** and R^6SiCl along with re-generated **1**.

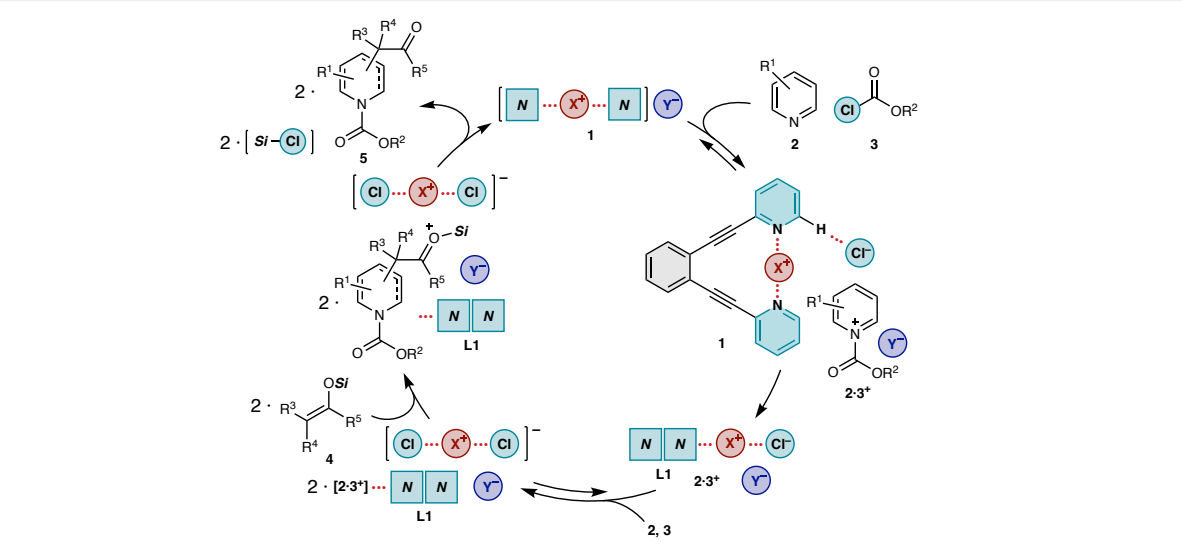

Fig. 6. Proposed catalytic cycle. *NN* indicates ligand **L1**, and *Si* indicates trimethyl- or *tert*-butyl dimethyl silyl groups.

To support the proposed mechanism, DFT calculations and UV-vis measurements were performed. Molecular electrostatic potential (MEP) of **1e** and [*N*···I···*N*]$^+$ was mapped on the isodensity surface based on the calculation of the density functional theory (DFT) calculations with the SMD18 model (Fig. 7a).[117] In both cases, MEP maps show that positive charges are delocalized on the pyridine ring of ligand, and not localized on the iodine atom. These results suggested that [*N*···X···*N*]Y would promote the reaction through charge-assisted noncovalent interactions, such as hydrogen bonding and anion–π interaction at the initial stage. Moreover, DFT calculations with the SMD18 model support formation of 3c4e X-bond from a pyridine nitrogen atom to chloride, *i.e.* transformation of [*N*···I···*N*]Cl to [*NN*···I···Cl] involving a Gibbs free energy change of –3.2 kcal/mol, and the transformation, [*NN*···I···Cl] + Cl^- ⟶ [*NN*] + [Cl···I···Cl]$^-$, with a Gibbs free energy change of –3.7

kcal/mol (Fig. 7b). Finally, UV-vis measurements were performed to identify the re-formation of [*N*···I···*N*]Ys for the catalytic cycle. The UV-vis spectrum of the crude reaction mixture shows absorption at 307 nm, which was similarly observed on the spectrum of **1e** (Fig. 7c), indicating that [Cl···X···Cl]$^-$ is transformed back to [*N*···X···*N*]$^+$. This can be explained by the robust catalytic activity of [*N*···X···*N*]Ys owing to the distinct feature of the charged 3c4e X-bond: partially covalent and strongly electrostatic interaction derived from halogen(I).

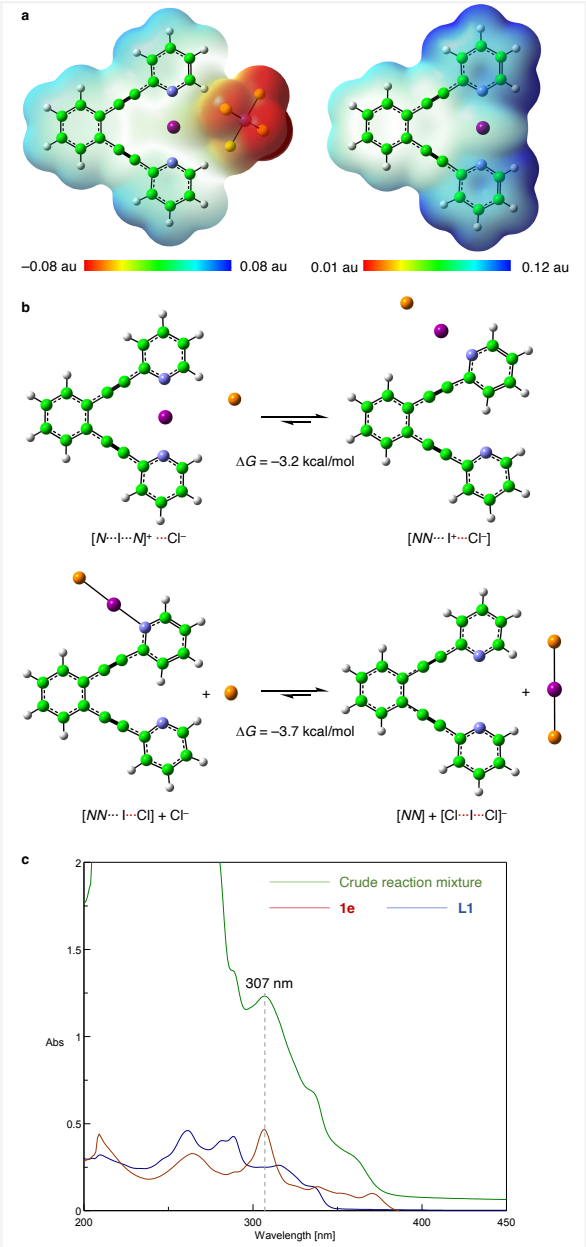

Fig. 7. Mechanistic studies of complexations. a). Molecular electrostatic potential map: [*N*···I···*N*]SbF_6 (**1e**), and [*N*···I···*N*]$^+$. SMD18(THF)/M06-2X-D3/6-311+G(d,p)-SDD-calculated electrostatic potentials on the

molecular surface. **b).** DFT calculation of [*N*···I···*N*]Cl → [*NN*···I···Cl], and [*NN*···I···Cl] + Cl^- → [*NN*] + $[Cl\cdots I\cdots Cl]^-$. **c).** UV-vis spectrum.

In summary, we demonstrate the use of bis-pyridine halogen(I) complexes (**1**: [*N*···X···*N*]Ys) with the 3c4e X-bond as highly effective anion-binding catalysts. [*N*···X···*N*]Ys accelerated nucleophilic dearomatization of pyridines quite seamlessly in significant yields under the sub-ppm level of catalyst loading. The charge-assisted H-bonding followed by the formation of $[Cl\cdots X\cdots Cl]^-$ enable [*N*···X···*N*]Ys to function as an anion-binding catalyst. The above results suggest that halogen(I) complexes may ultimately be applied broadly in catalysis. The present study also represents the first successful use of the N···X-based 3c4e X-bond catalyst and shows its potential use in other catalytic reactions, whether through Lewis acid or Brønsted acid catalysis. Studies on the application of [*N*···X···*N*]Y catalysts to other reactions, and the catalytic asymmetric version of this system are ongoing, and will be reported in due course.

Methods

General procedures for the nucleophilic dearomatization of pyridines

Pyridine (32 μL, 0.400 mmol, 1.0 equiv.) was dissolved in THF (8 mL) and stirred at 0 °C for 10 min. Phenyl chloroformate (55 μL, 0.420 mmol, 1.1 equiv.) was added and stirred for an additional 30 min. A catalyst (0.20 μmol, 0.05 mol%) was added to the solution, which was then stirred for 5 min. Methyl trimethylsilyl dimethylketene acetal (0.120 mL, 0.600 mmol, 1.5 equiv.) was added to the reaction mixture. The mixture was stirred for 1 h. The reaction mixture was quenched with saturated aqueous $NaHCO_3$ (20 mL), then the two phases were separated. The aqueous phase was extracted with diethyl ether (10 mL × 3). The combined organic phases were washed with NaOH (2 M, 10 mL) and brine (10 mL), then dried over Na_2SO_4 and concentrated under reduced pressure after filtration. The crude product was purified by silica gel column chromatography (ethyl acetate / hexane = 1:8) to yield a slight yellow oil (99.3 mg, 0.330 mmol, 82%).

Data availability

All data in this study are provided in the supplementary information. The X-ray crystallographic data can be accessed from the Cambridge Crystallographic Data Center (CCDC) under accession code CCDC-2152341 ([^{F4}*N*–I–*N*][Cl–I–Cl]), CCDC-2152342 (**1d**), CCDC-2152343 (**1e**), CCDC-2152344 (**5m**), CCDC-2152345 (**L1**), CCDC-2152346 ([NN]·2ICl), CCDC-2152347 (**L2**), and CCDC-2152348 ([^{F4}*N*–I–*N*][Cl–I–Cl] and [Cl–I–^{F4}*NN*–I–Cl]).

References

1. Dalko, P. I. & Moisan, L. In the golden age of organocatalysis. *Angew. Chem. Int. Ed. Engl*. **43**, 5138–5175 (2004).
2. List, B. Introduction: Organocatalysis. *Chem. Rev*. **107**, 5413–5415 (2007).
3. Gaunt, M. J., Johansson, C. C. C., McNally, A. & Vo, N. T. Enantioselective organocatalysis. In. *Drug Discovery Today* **12**, 8–27 (2007).
4. Barbas, C. F. Organocatalysis Lost: Modern Chemistry, Ancient Chemistry, and an Unseen Biosynthetic Apparatus. *Angew. Chem., Int. Ed.* **47**, 42–47 (2008).
5. MacMillan, D. W. The advent and development of organocatalysis. *Nature* **455**, 304–308 (2008).
6. Jacobsen, E. N. & MacMillan, D. W. Organocatalysis. *Proc. Natl. Acad. Sci*. **107**, 20618–20619 (2010).
7. Mahlau, M. & List, B. Asymmetric Counteranion-Directed Catalysis: Concept, Definition, and Applications. *Angew. Chem. Int. Ed*. **52**, 518–533 (2013).
8. Brak, K. & Jacobsen, E. N. Asymmetric Ion-Pairing Catalysis. *Angew. Chem. Int. Ed*. **52**, 534–561 (2013).
9. Parmar, D., Sugiono, E., Raja, S. & Rueping, M. Complete Field Guide to Asymmetric BINOL-Phosphate Derived Brønsted Acid and Metal Catalysis: History and Classification by Mode of Activation; Brønsted Acidity, Hydrogen Bonding, Ion Pairing, and Metal Phosphates. *Chem. Rev*. **114**, 9047‑9153 (2014).
10. Akiyama, T. & Mori, K. Stronger Brønsted Acids: Recent Progress. *Chem. Rev*. **115**, 9277‑9306 (2015).
11. Holland, M. C. & Gilmour, R. Deconstructing covalent organocatalysis. *Angew. Chem., Int. Ed*. **54**, 3862–3871 (2015).
12. Schreiner, P. R. Metal-Free Organocatalysis through Explicit Hydrogen Bonding Interactions. *Chem. Soc. Rev.* **32**, 289–296 (2003).
13. Doyle, A. G. & Jacobsen, E. N. Small-Molecule H-Bond Donors in Asymmetric Catalysis. *Chem. Rev*. **107**, 5713–5743 (2007).
14. Chauhan, P., Mahajan, S., Kaya, U., Hack, D. & Enders, D. Bifunctional Amine-Squaramides: Powerful Hydrogen-Bonding Organocatalysts for Asymmetric Domino/Cascade Reactions. *Adv. Synth. Catal*. **357**, 253–281 (2015).
15. Mahmudov, K. T., Kopylovich, M. N., Guedes da Silva, M. F. C. & Pombeiro, A. J. L. *Noncovalent Interactions in Catalysis*; Royal Society of Chemistry, UK (2019).
16. Erdélyi, M. Halogen bonding in solution. *Chem. Soc. Rev*. **41**, 3547–3557 (2012).
17. Beale, T. M., Chudzinski, M. G., Sarwar, M. G. & Taylor, M. S. Halogen bonding in solution: thermodynamics and applications. *Chem. Soc. Rev.* **42**, 1667–1680 (2013).
18. Jentzsch, A. V. Applications of halogen bonding in solution. *Pure Appl. Chem*. **87**, 15–41 (2015).

19. Tepper, R. & Schubert, U. S. Halogen bonding in solution: anion recognition, templated self-assembly, and organocatalysis. *Angew. Chem. Int. Ed*. **57**, 6004–6016 (2018).
20. Carlsson, A.-C. C., Veiga, A. X. Z. & Erdélyi, M. "Halogen Bonding in Solution" in Halogen Bonding II: Impact on Materials Chemistry and Life Sciences; Metrangolo, P. and Resnati, G. eds., 2015. Springer Cham Heidelberg New York Dordrecht London *Top. Curr. Chem*. **359**, 49–76 (2015).
21. Wilcox, S., Herrebout, W. & Erdélyi, M. "Spectroscopy of Halogen Bonding in Solution" in Halogen Bonding in Solution; Huber, S. M. ed., 2021, Wiley-VCH Verlag GmbH & Co. KGaA, pp. 153–194.
22. Schindler, S. & Huber, S. M. "Halogen Bonds in Organic Synthesis and Organocatalysis" in Halogen Bonding II: Impact on Materials Chemistry and Life Sciences; Metrangolo, P. and Resnati, G. eds., 2015. Springer Cham Heidelberg New York Dordrecht London *Top. Curr. Chem*. **359**, 167–203 (2015).
23. Sutar, R. & Huber, S. M. Catalysis of organic reactions through halogen bonding. *ACS Catal*. **9**, 9622–9639 (2019).
24. Bamberger, J., Ostler, F. & Mancheño, O. G. Frontiers in halogen and chalcogen-bond donor organocatalysis. *ChemCatChem* **11**, 5198–5211 (2019).
25. Breugst, M. & Koenig, J. J. σ-Hole interactions in catalysis. *Eur. J. Org. Chem*. 5473–5487 (2020).
26. Yang, H., & Wong, M. W. Application of halogen bonding to organocatalysis: a theoretical perspective. *Molecules* **25**, 1045 (2020).
27. Sutar, R. L. "Halogen Bonding in Organocatalysis" in Halogen Bonding in Solution; Huber, S. M. ed., 2021, Wiley-VCH Verlag GmbH & Co. KGaA, pp. 269–306.
28. Bruckmann, A., Pena, M. A. & Bolm, C. Organocatalysis through halogen-bond activation. *Synlett* 900–902 (2008).
29. Walter, S. M., Kniep, F., Herdtweck, E. & Huber, S. M. Halogen-Bond-Induced Activation of a Carbon–Heteroatom Bond. *Angew. Chem. Int. Ed*. **50**, 7187–7191 (2011).
30. Jungbauer, S. H., Walter, S. M., Schindler, S., Rout, L., Kniep, F. & Huber, S. M. Activation of a carbonyl compound by halogen bonding. *Chem. Commun.* **50**, 6281–6284 (2014).
31. He, W., Ge, Y.-C. & Tan, C.-H. Halogen-Bonding-Induced Hydrogen Transfer to C=N Bond with Hantzsch Ester. *Org. Lett.* **16**, 3244–3247 (2014).
32. Saito, M., Tsuji, N., Kobayashi, Y. & Takemoto, Y. Direct Dehydroxylative Coupling Reaction of Alcohols with Organosilanes through Si‑X Bond Activation by Halogen Bonding. *Org. Lett*. **17**, 3000‑3003 (2015).
33. Takeda, Y., Hisakuni, D., Lin, C.-H. & Minakata, S. 2-Halogenoimidazolium Salt Catalyzed Aza-Diels–Alder Reaction through Halogen-bond Formation *Org. Lett*. **17**, 318–321 (2015).

34. Zhang, Y., Han, J. & Liu, Z.-J. Diaryliodonium Salts as Efficient Lewis Acid Catalysts for Direct Three Component Mannich Reactions. *RSC Adv*. **5**, 25485–25488 (2015).
35. Zeng, Y., Li, G. & Hu, J. Diphenyliodonium-Catalyzed Fluorination of Arynes: Synthesis Ofortho-Fluoroiodoarenes. *Angew. Chem. Int. Ed.* **54**, 10773–10777 (2015).
36. Heinen, F., Engelage, E., Dreger, A., Weiss, R. & Huber, S. M. Iodine(III) Derivatives as Halogen Bonding Organocatalysts. *Angew. Chem. Int. Ed*. **57**, 3830–3833 (2018).
37. Wolf, J., Huber, F., Erochok, N., Heinen, F., Guérin, V., Legault, C. Y., Kirsch, S. F. & Huber, S. M. Activation of a Metal-Halogen Bond by Halogen Bonding. *Angew. Chem. Int. Ed*. **59**, 16496–16500 (2020).
38. Haraguchi, R., Nishikawa, T., Kanazawa, A. & Aoshima, S. Metal-Free Living Cationic Polymerization Using Diaryliodonium Salts as Organic Lewis Acid Catalysts. *Macromolecules* **53**, 4185–4192 (2020).
39. Heinen, F., Reinhard, D. L., Engelage, E. & Huber, S. M. A Bidentate Iodine(III)-Based Halogen-Bond Donor as a Powerful Organocatalyst. *Angew. Chem. Int. Ed*. **60**, 5069–5073 (2021).
40. Sutar, R. L., Engelage, E., Stoll, R. & Huber, S. M. Bidentate Chiral Bis(Imidazolium)-Based Halogen-Bond Donors: Synthesis and Applications in Enantioselective Recognition and Catalysis. *Angew. Chem., Int. Ed*. **59**, 6806–6810 (2020).
41. Kuwano, S., Suzuki, T., Hosaka, Y. & Arai, T. A chiral organic base catalyst with halogen-bonding-donor functionality: asymmetric Mannich reactions of malononitrile with N-Boc aldimines and ketimines. *Chem. Commun.* **54**, 3847–3850 (2018).
42. Kuwano, S., Nishida, Y., Suzuki, T. & Arai, T. Catalytic Asymmetric Mannich-Type Reaction of Malononitrile with N-Boc α-Ketiminoesters Using Chiral Organic Base Catalyst with Halogen Bond Donor Functionality. *Adv. Synth. Catal.* **362**, 1674–1678 (2020).
43. Kuwano, S., Ogino, E. & Arai, T. Enantio- and diastereoselective double Mannich reaction of malononitrile with N-Boc imines using quinine-derived bifunctional organoiodine catalyst. *Org. Biomol. Chem*. **19**, 6969–6973 (2021).
44. Zong, L., Ban, X., Kee, C. W. & Tan, C. H. Catalytic Enantioselective Alkylation of Sulfenate Anions to Chiral Heterocyclic Sulfoxides Using Halogenated Pentanidium Salts. *Angew. Chem., Int. Ed*. **53**, 11849–11853 (2014).
45. Chan, Y.-C. & Yeung, Y.-Y. Halogen-Bond-Catalyzed Addition of Carbon-Based Nucleophiles to N-Acylimminium ions. *Org. Lett.* **21**, 5665–5669 (2019).
46. Ostler, F., Piekarski, D. G., Danelzik, T., Taylor, M. S. & Mancheño, O. G. Neutral Chiral Tetrakis-Iodo-Triazole Halogen-Bond Donor for Chiral Recognition and Enantioselective Catalysis. *Chem. Eur. J*. **27**, 2315–2320 (2021).
47. Yoshida, Y., Mino, T. & Sakamoto, M. Chiral Hypervalent Bromine(III) (Bromonium Salt): Hydrogen- and Halogen-Bonding Bifunctional Asymmetric Catalysis by Diaryl-λ 3-Bromanes. *ACS Catal*. **11**, 13028–13033 (2021).

48. Nugent, B. M., Yoder, R. A. & Johnston, J. N. Chiral Proton Catalysis: A Catalytic Enantioselective Direct Aza-Henry Reaction. *J. Am. Chem. Soc.* **126**, 3418–3419 (2004).
49. Hess, A. S., Yoder, R. A. & Johnston, J. N. Chiral Proton Catalysis: pKa Determination for a BAM-HX Brønsted Acid. *Synlett* 147–149 (2006).
50. Singh, A., Yoder, R. A., Shen, B. & Johnston, J. N. Chiral Proton Catalysis: Enantioselective Brønsted Acid Catalyzed Additions of Nitroacetic Acid Derivatives as Glycine Equivalents. *J. Am. Chem. Soc*. **129**, 3466–3467 (2007).
51. Takenaka, N., Chen, J., Captain, B., Sarangthem, R. S. & Chandrakumar, A. Helical Chiral 2-Aminopyridinium Ions: A New Class of Hydrogen Bond Donor Catalysts. *J. Am. Chem. Soc.* **132**, 4536–4537 (2010).
52. Peng, Z. & Takenaka, N. Applications of Helical-Chiral Pyridines as Organocatalysts in Asymmetric Synthesis. *Chem Rec* **13**, 28–42 (2013).
53. Perrin, C. L. Symmetry of hydrogen bonds in solution. *Pure Appl. Chem*. **81**, 571-578 (2009).
54. Perrin, C. L. Are Short, Low-Barrier Hydrogen Bonds Unusually Strong? *Acc. Chem. Res*. **43**, 1550-1557 (2010).
55. Wang, Y. & Yu, Z.-X. Symmetric C···H···C Hydrogen Bonds Predicted by Quantum Chemical Calculations. *J. Org. Chem*. **85**. 397–402 (2020).
56. Perrin, C. L & Wu, Y. Symmetry of Hydrogen Bonds in Two Enols in Solution. *J. Am. Chem. Soc.* **141**, 4103–4107 (2019).
57. Kochanek, S. E., Clymer, T. M., Pakkala, V. S., Hebert, S. P., Reeping, K., Firestine, S. M. & Evanseck, J. D. Intramolecular Charge-Assisted Hydrogen Bond Strength in Pseudochair Carboxyphosphate. *J. Phys. Chem. B*. **119**, 1184–1191 (2015).
58. Perrin, C. L & Burke, K. D. Variable-Temperature Study of Hydrogen-Bond Symmetry in Cyclohexene-1,2-dicarboxylate Monoanion in Chloroform-*d*. *J. Am. Chem. Soc.* **136**, 4355–4362 (2014).
59. Masuda, Y., Mori, Y., & Sakurai, K. Effects of Counterion and Solvent on Proton Location and Proton Transfer Dynamics of N–H···N Hydrogen Bond of Monoprotonated 1,8-Bis(dimethylamino)naphthalene. *J. Phys. Chem. A*. **117**, 10576–10587 (2013).
60. Erdélyi, M. Halogen bonding in solution. *Chem. Soc. Rev*. **41**, 3547–3557 (2012).
61. Carlsson, A.-C. C., Veiga, A. X. Z. & Erdélyi, M. "Halogen Bonding in Solution" in Halogen Bonding II: Impact on Materials Chemistry and Life Sciences; Metrangolo, P. and Resnati, G. eds., 2015. Springer Cham Heidelberg New York Dordrecht London *Top. Curr. Chem.* **359**, 49–76 (2015).
62. Rissanen, K. & Haukka, M. "Halonium Ions as Halogen Bond Donors in the Solid State [XL2]Y Complexes" in Halogen Bonding II: Impact on Materials Chemistry and Life Sciences; Metrangolo, P. and Resnati, G. eds., 2015. Springer Cham Heidelberg New York Dordrecht London *Top. Curr. Chem.* **359**, 77–90 (2015).

63. Turunen, L. & Erdélyi, M. Halogen bonds of halonium ions. *Chem. Soc. Rev.*, **49**, 2688–2700 (2020).
64. Carlsson, A.-C. C., Gräfenstein, J., Budnjo, A., Laurila, J. L., Bergquist, J., Karim, A., Kleinmaier, R., Brath, U. & Erdélyi, M. Symmetric Halogen Bonding Is Preferred in Solution. *J. Am. Chem. Soc.* **134**, 5706 (2012).
65. Carlsson, A.-C. C., Gräfenstein, J., Laurila, J. L., Bergquist, J. & Erdélyi, M. Symmetry of $[N\text{-}X\text{-}N]^+$ Halogen Bonds in Solution. *Chem. Commun*. **48**, 1458–1460 (2012).
66. Carlsson, A.-C. C., Uhrbom, M., Karim, A. Brath, U. Gräfenstein, J. & Erdélyi, M. Solvent effects on halogen bond symmetry. *CrystEngComm* **15**, 3087–3092 (2013).
67. Karim, A., Reitti, M., Carlsson, A.-C. C., Gräfenstein, J. & Erdélyi, M. The Nature of $[N\text{-}Cl\text{-}N]^+$ and $[N\text{-}F\text{-}N]^+$ Halogen Bonds in Solution. *Chem. Sci*. **5**, 3226–3233 (2014).
68. Hakkert, S. B. & Erdélyi, M. Halogen Bond Symmetry: The N-X- N Bond. *J. Phys. Org. Chem*. **28**, 226–223 (2015).
69. Bedin, M., Karim, A., Reitti, M., Carlsson, A.-C. C., Topic, F., Cetina, M., Pan, F. F., Havel, V., Al-Ameri, F., Sindelar, V., Rissanen, K., Gräfenstein, J. & Erdélyi, M. Counterion Influence on the N-I-N Halogen Bond. *Chem. Sci*. **6**, 3746–3756 (2015).
70. Carlsson, A.-C. C., Mehmeti, K., Uhrbom, M., Karim, A., Bedin, M., Puttreddy, R., Kleinmaier, R., Neverov, A. A., Nekoueishahraki, B., Gräfenstein, J., Rissanen, K. & Erdélyi, M. Substituent Effects on the $[N\text{-}I\text{-}N]^+$ Halogen Bond. *J. Am. Chem. Soc*. **138**, 9853–9863 (2016).
71. Lindblad, S., Mehmeti, K., Veiga, A. X., Nekoueishahraki, B., Gräfenstein, J. & Erdélyi, M. Halogen Bond Asymmetry in Solution. *J. Am. Chem. Soc.* **140**, 13503–13513 (2018).
72. Vanderkooy, A., Gupta, A. K., Földes, T., Lindblad, S., Orthaber, A., Pápai, I. & Erdélyi, M. Halogen Bonding Helicates Encompassing Iodonium Cations. *Angew. Chem., Int. Ed. Engl.* **58**, 9012–9016 (2019).
73. Reiersølmoen, A., Battaglia, S., Øien-Ødegaard, S., Gupta, A. K., Fiksdahl, A., Lindh, R. & Erdélyi, M. Symmetry of three-center, four-electron bonds. *Chem. Sci*. **11**, 7979–7990 (2020).
74. Lindblad, S., Németh, F. B., Földes, T., Vanderkooy, A., Pápai, I. & Erdélyi, M. O-I-O Halogen Bond of Halonium Ions. *Chem. Commun* **56**, 9671–9674 (2020).
75. Heiden, von der D. Rissanen, K. & Erdélyi, M. Asymmetric $[N–I–N]^+$ halonium complexes in solutions? *Chem. Commun*. **56**, 14431–14434 (2020).
76. Heiden, von der D. Németh, F. B., Andreasson, M., Sethio, D., Pápai, I., & Erdélyi, M. Are bis(pyridine)iodine(I) complexes applicable for asymmetric halogenation? *Org. Biomol. Chem*. **19**, 8307–8323 (2021).
77. Lindblad, S., Boróka Németh, F., Földes, T., Heiden, D., Vang, H. G., Driscoll, Z. L., Gonnering, E. R., Pápai, I., Bowling, N., & Erdélyi, M. The Influence of Secondary Interactions on the $[N–I–N]^+$ Halogen Bond. *Chem. Eur. J.* **27**, 13748–13756 (2021).

78. Barluenga, J. Transferring iodine: more than a simple functional group exchange in organic synthesis. *Pure Appl. Chem.* **71**, 431–436 (1999).
79. Justin, M., Amber, L. & Benjamin, G. SAFE AND SCALABLE PREPARATION OF BARLUENGA'S REAGENT. *Org. Synth*. **87**, 288–298 (2010).
80. Tsuji, N., Kobayashi, Y. & Takemoto, Y. Electrophilic iodine(i) compounds induced semipinacol rearrangement via C–X bond cleavage. *Chem. Commun*. **50**, 13691–13694 (2014).
81. Kiyokawa, K., Kosaka, T. & Minakata, S. Metal-Free Aziridination of Styrene Derivatives with Iminoiodinane Catalyzed by a Combination of Iodine and Ammonium Iodide *Org. Lett*. **15**, 18, 4858–4861 (2013).
82. Zhang, Z. & Schreiner, P. R. (Thio)urea organocatalysis—What can be learnt from anion recognition? *Chem. Soc. Rev.* **38**, 1187–1198 (2009).
83. Beckendorf, S., Asmus, S. & Mancheño, O. G. H-Donor Anion Acceptor Organocatalysis—The Ionic Electrophile Activation Approach. *ChemCatChem* **4**, 926–936 (2012).
84. Seidel, D. The Anion-Binding Approach to Catalytic Enantioselective Acyl Transfer. *Synlett* **25**, 783–794 (2014)
85. Visco, M. D., Attard, J. Guan, Y. & Mattson, A. E. Anion-binding catalyst designs for enantioselective synthesis. *Tetrahedron Lett*. **58**, 2623–2684 (2017).
86. Schifferer, L. Stinglhamer, M. Kaur, K. & Mancheño, O. G. Halides as versatile anions in asymmetric anion-binding organocatalysis, *Beilstein J. Org. Chem*. **17**, 2270–2286 (2021).
87. Suzaki, Y., Saito, T., Ide, T., & Osakada, K. A rhomboid-shaped organic host molecule with small binding space. Unsymmetrical and symmetrical inclusion of halonium ions. *Dalton Trans*. **43**, 6643–6649 (2014).
88. Bull, J. A., Mousseau, J. J., Pelletier, G. & Charette, A. B. Synthesis of Pyridine and Dihydropyridine Derivatives by Regio- and Stereoselective Addition to N-Activated Pyridines. *Chem. Rev.* **112**, 2642–2713 (2012).
89. Ding, Q., Zhou, X. & Fan, R. Recent Advances in Dearomatization of Heteroaromatic Compounds. *Org. Biomol. Chem.* **12**, 4807–4815 (2014).
90. Bertuzzi, G., Bernardi, L. & Fochi, M. Nucleophilic Dearomatization of Activated Pyridines. *Catalysts* **8**, 632 (2018).
91. Sowmiah, S., Esperança, J. M. S. S., Rebelo, L. P. N. & Afonso, C. A. M. Pyridinium Salts: From Synthesis to Reactivity and Applications. *Org. Chem. Front*. **5**, 453–493 (2018).
92. Zhou, F.-Y. & Jiao, L. Recent Developments in Transition-Metal-Free Functionalization and Derivatization Reactions of Pyridines. *Synlett* **32**, 159–178 (2021).
93. Taylor, M. S., Tokunaga, N. & Jacobsen, E. N. Enantioselective Thiourea-Catalyzed Acyl- Mannich Reactions of Isoquinolines. *Angew. Chem., Int. Ed*. **44**, 6700–6704 (2005).

94. Schafer, A. G., Wieting, J. M., Fisher, T. J. & Mattson, A. E. Chiral Silanediols in Anion-Binding Catalysis. *Angew. Chem., Int. Ed.* **52**, 11321–11324 (2013).
95. Zurro, M., Asmus, S., Beckendorf, S., Mück-Lichtenfeld, C. & Mancheño, O. G. Chiral Helical Oligotriazoles: New Class of Anion-Binding Catalysts for the Asymmetric Dearomatization of Electron-Deficient N-Heteroarenes. *J. Am. Chem. Soc.* **136**, 13999–14002 (2014).
96. Mancheño, O. G., Asmus, S., Zurro, M. & Fischer, T. Highly Enantioselective Nucleophilic Dearomatization of Pyridines by Anion-Binding Catalysis. *Angew. Chem., Int. Ed*. **54**, 8823–8827 (2015).
97. Wieting, J. M., Fisher, T. J., Schafer, A. G., Visco, M. D., Gallucci, J. C. & Mattson, A. E. Preparation and Catalytic Activity of BINOL-Derived Silanediols. *Eur. J. Org. Chem.* 525–533 (2015).
98. Shirakawa, S., Liu, S., Kaneko, S., kumatabara, Y., Fukuda, A., Omagari, Y. & Maruoka, K. Tetraalkylammonium Salts as Hydrogen-Bonding Catalysts. *Angew. Chem. Int. Ed.* **54**, 15767–15770 (2015).
99. Choudhury, A. R. & Mukherjee, S. Enantioselective dearomatization of isoquinolines by anion-binding catalysis en route to cyclic α-aminophosphonates. *Chem. Sci*. **7**, 6940–6945 (2016).
100. Kaneko, S., Kumatabara, Y., Shimizu, S., Maruoka, K & Shirakawa, S. Hydrogen-bonding catalysis of sulfonium salts. *Chem. Commun*. **53**, 119–122 (2017).
101. Fischer, T., Duong, Q.-N., Mancheño, O. G. Triazole-Based Anion-Binding Catalysis for the Enantioselective Dearomatization of N-Heteroarenes with Phosphorus Nucleophiles. *Chem. Eur. J*. **23**, 5983–5987 (2017).
102. Wolf, F. F., Meudörfl, J.-M. & Goldfuss, B. Hydrogen-bonding cyclodiphosphazanes: superior effects of 3,5-(CF3)2-substitution in anion-recognition and counter-ion catalysis. *New J. Chem.* **42**, 4854–4870 (2018).
103. Duong, Q.-N., Schifferer, L. & Mancheño, O. G. Nucleophile Screening in Anion-Binding Reissert-Type Reactions of Quinolines with Chiral Tetrakis(triazole) Catalysts. *Eur. J. Org. Chem.* 5452–5461 (2019).
104. Ostler, F., Piekarski, D. G., Danelzik, T., Taylor, M. S. & Mancheño, O. G. Neutral Chiral Tetrakis-Iodo-Triazole Halogen-Bond Donor for Chiral Recognition and Enantioselective Catalysis. *Chem. Eur. J.* **27**, 2315–2320 (2021).
105. Matador, E., Iglesias-Sigüenza, J., Monge, D., Merino, P., Fernández, R. & Lassaletta, J. M. Enantio- and Diastereoselective Nucleophilic Addition of N-tert-Butylhydrazones to Isoquinolinium Ions through Anion-Binding Catalysis. *Angew. Chem. Int. Ed*. **60**, 5096–5101 (2021).

106. Gómez-Martínez, M., Pérez-Aguilar, M. C., Piekarski, D. G., Daniliuc, C. G. & Mancheño, O. G. N,N-Dialkylhydrazones as Versatile Umpolung Reagents in Enantioselective Anion-Binding Catalysis. *Angew. Chem. Int. Ed*. **60**, 5102–5107 (2021).
107. Kotke, M. & Schreiner, P. R. Acid-free, organocatalytic acetalization. *Tetrahedron* **62**, 434–439 (2006).
108. Asmus, S., Beckendorf, S., Zurro, M., Mück-Lichtenfeld, C. & Mancheño, O. G. Influence of the Substitution and Conformation of C–H-Bond-Based Bis-Triazole Acceptors in Anion-Binding Catalysis. *Chem. Asian. J*. **9**, 2178–2186 (2014).
109. Berkessel, A., Das, S., Pekel, D. & Neudörfl, J.-M. Anion-Binding Catalysis by Electron-Deficient Pyridinium Cations. *Angew. Chem. Int. Ed*, **53**, 11660–11664 (2014).
110. Popov, A. I. & Pflaum, R. T. Studies on the Chemistry of Halogens and of Polyhalides. X. The reactions of iodine monochloride with pyridine and with 2,20-bipyridine. *J. Am. Chem. Soc*. **79**, 570–572 (1957).
111. Popov, A.I. & Rygg, R.H. Studies on the Chemistry of Halogens and of Polyhalides. XI. Molecular complexes of Pyridine, 2-Picoline and 2,6-Lutidine with Iodine and Iodine Halides. *J. Am. Chem. Soc*. **79**, 4622–4625 (1957).
112. Zíngaro, R. A. & Tolberg, W. E. Infrared Spectra of Pyridine Coor- dinated Iodine (I) Salts. *J. Am. Chem. Soc*. **81**, 1353–1357 (1959).
113. Creighton, J. A., Haque, I. & Wood, J. L. The Iododipyridinium Ion. *Chem. Commun.*, 229 (1966).
114. Haque, I. & Wood, J. L. The Infra-Red Spectra of Pyridine-Halogen Complexes. *Spectrochim. Acta Part A* **23**, 959–967 (1967).
115. Jones, B., Moody, G. J. & Thomas, J. D. R. N-Iodopyridinium Dichloroiodate(I). *Inorg. Chem.* **9**, 114–119 (1970).
116. Tassaing, T. & Besnard, M. Ionization reaction in iodine/pyridine solutions: what can we learn from conductivity measurements, far-infrared spectroscopy, and Raman scattering? *J. Phys. Chem. A*. **101**, 2803–2808 (1997).
117. Engelage, E., Schulz, N., Heinen, F., Huber, S. M., Truhlar, D. G. & Cramer, C. J. Refined SMD Parameters for Bromine and Iodine Accurately Model Halogen-Bonding Interactions in Solution. *Chem. Eur. J.* **24**, 15983–15987 (2018).

Acknowledgements
This work was partially supported by the Astellas Foundation for Research on Metabolic Disorders, the Suzuken memorial foundation, and the Grand-in-Aid for Transformative Research Areas (A) 21A204 Digitalization-driven Transformative Organic Synthesis (Digi-TOS) from the Ministry of Education, Culture, Sports, Science & Technology, Japan. We sincerely thank Prof. Susumu Saito and Dr. Kin-ichi Oyama (Nagoya University) for the CSI-MS measurements. We also appreciate Prof. Yasuhiro Uozumi and Prof. Toshiaki Mase

(Institute for Molecular Science, JST) for helpful discussions. N.M. and T.F. gratefully acknowledge JST-ACCEL for their financial support.

Author contributions

N.M. conceived and directed the project, and N.M., S.O., and T.F. co-wrote the manuscript. S.O., T.F., and Y.M. developed the reaction, and S.O. and T.F. contributed equally. T.S. performed the DFT calculation, and M.K. and N.O. performed part of the experiments in the mechanistic studies.

Competing interests

The authors declare no competing interests.